

Published in final edited form as:

Biochem J. 2008 May 1; 411(3): 647–655. doi:10.1042/BJ20071084.

Akt substrate TBC1D1 regulates GLUT1 expression through the mTOR pathway in 3T3-L1 adipocytes

Qiong L. Zhou¹, Zhen Y. Jiang¹, John Holik, Anil Chawla, G. Nana Hagan, John Leszyk, and Michael P. Czech²

Programme in Molecular Medicine, University of Massachusetts Medical School, 373 Plantation Street, Worcester, MA 01605, U.S.A.

Abstract

Multiple studies have suggested that the protein kinase Akt/PKB (protein kinase B) is required for insulin-stimulated glucose transport in skeletal muscle and adipose cells. In an attempt to understand links between Akt activation and glucose transport regulation, we applied mass spectrometry-based proteomics and bioinformatics approaches to identify potential Akt substrates containing the phospho-Akt substrate motif RXXRXXpS/T. The present study describes the identification of the Rab GAP (GTPase-activating protein)-domain containing protein TBC1D1 [TBC (Tre-2/Bub2/Cdc16) domain family, member 1], which is closely related to TBC1D4 [TBC domain family, member 4, also denoted AS160 (Akt substrate of 160 kDa)], as an Akt substrate that is phosphorylated at Thr⁵⁹⁰. RNAi (RNA interference)-mediated silencing of TBC1D1 elevated basal deoxyglucose uptake by approx. 61% in 3T3-L1 mouse embryo adipocytes, while the suppression of TBC1D4 and RapGAP220 under the same conditions had little effect on basal and insulin-stimulated deoxyglucose uptake. Silencing of TBC1D1 strongly increased expression of the GLUT1 glucose transporter but not GLUT4 in cultured adipocytes, whereas the decrease in TBC1D4 had no effect. Remarkably, loss of TBC1D1 in 3T3-L1 adipocytes activated the mTOR (mammalian target of rapamycin)-p70 S6 protein kinase pathway, and the increase in GLUT1 expression in the cells treated with TBC1D1 siRNA (small interfering RNA) was blocked by the mTOR inhibitor rapamycin. Furthermore, overexpression of the mutant TBC1D1-T590A, lacking the putative Akt/PKB phosphorylation site, inhibited insulin stimulation of p70 S6 kinase phosphorylation at Thr³⁸⁹, a phosphorylation induced by mTOR. Taken together, our data suggest that TBC1D1 may be involved in controlling GLUT1 glucose transporter expression through the mTOR-p70 S6 kinase pathway.

Keywords

Akt substrate of 160 kDa (AS160); GLUT1; GTPase-activating protein (GAP); insulin signalling; mammalian target of rapamycin (mTOR); protein kinase B (PKB)/Akt

INTRODUCTION

Akt/PKB (protein kinase B) is a key intermediate in signalling pathways initiated by hormones and growth factors that activate PI3K (phosphoinositide 3-kinase) [1–4]. Three Akt/PKB isoforms are phosphorylated and activated by two upstream protein kinases in response to the formation of PtdIns(3,4,5)P₃. Of these upstream kinases, one is PDK1 (phosphoinositide-dependent protein kinase 1) [1–4], while the other is mTOR (mammalian target of rapamycin)

in complex with the protein rictor [5]. Numerous studies have demonstrated that activation of Akt/PKB is involved in insulin's metabolic and mitogenic functions including the regulation of gene expression, glucose transport, glycogen synthesis, protein synthesis, cell survival and cell growth [1–4]. Activated Akt/PKB regulates cellular functions through phosphorylation of serine and threonine residues in the motif RXXRXXS/T of downstream target proteins [6–8]. Multiple Akt/PKB substrates have been discovered, such as transcription factor FOXO (forkhead box O) proteins [9–12], the pro-apoptotic factor Bad [13], IκB (inhibitory κB) kinase [14,15], the mito-genic factor Raf1 [16–18], the p53 negative regulator Mdm2 [17,18], the cyclin-dependent kinase inhibitors p27kip1 [19–21] and p21cip1 [22], endothelial nitric oxide synthase [23,24], glycogen synthase kinase-3 [25], WNK1 (protein kinase with no lysine 1) [26,27] and the GAPs (GTPase-activating proteins) tuberous sclerosis complex TSC2 (tuberous sclerosis complex 2) [28,29], AS160 (Akt substrate of 160 kDa) [30] and many others [31,32].

Previously, proteins with GAP domains and activity have been identified as Akt/PKB substrates [33]. For example, the RabGAP TBC1D4 [TBC (Tre-2/Bub2/Cdc16) domain family, member 4; also known as AS160] was discovered by Lienhard and co-workers as an Akt/PKB substrate in adipocytes that further work showed has a role in part of the signalling cascade that mediates GLUT4 glucose transporter translocation to the plasma membrane [34–36]. Another example is TSC2, a specific GAP for the small GTPase Rheb [37–39]. Akt phosphorylates TSC2 at Thr¹⁴⁶² and inhibits its GAP activity [28,29,40], leading to the activation of the Rheb GTPase and subsequent activation of the protein kinase mTOR by a mechanism not yet clearly defined [41–43]. It is well established that mTOR activates protein synthesis through the activation of p70 S6 kinase and regulation of the eIF4F [eIF (eukaryotic initiation factor) 4F] complex [44,45]. In this pathway, mTOR phosphorylates the Thr³⁸⁹ residue in the hydrophobic motif of the p70 S6 kinase and activates the kinase [46–48]. In turn, p70 S6 kinase subsequently activates the S6 protein of the 40S ribosomal subunit by phosphorylating multiple residues including Ser²³⁵, Ser²³⁶, Ser²⁴⁰ and Ser²⁴⁴, which leads to an increase in mRNA translation [49]. Active p70 S6 kinase also stimulates translation by phosphorylating several other substrates involved in protein synthesis such as eIF4B, eEF2K (eukaryotic elongation factor 2-kinase) and SKAR (S6 kinase 1 Aly/REF-like target) [50]. In addition, mTOR induces hyperphosphorylation of 4E-BP1 (eIF4E-binding protein 1) and disrupts the binding of 4E-BP1 to eIF4E, which in turn mediates the binding of eIF4F, a large protein complex, to the 5' cap structure of mRNAs [51–53]. Thus, Akt-mediated activation of the mTOR pathway increases the translation of specific mRNA subpopulations.

It is likely that other unknown Akt/PKB effectors may be involved in insulin-induced protein synthesis and glucose transport. To search for such new Akt/PKB substrates, we applied an MS-based proteomics approach to identify potential candidates enriched by immunoprecipitation with a polyclonal antibody against the PAS (phospho-Akt/PKB substrate) motif RXXRXXpS/ T [27,54]. We also applied the web-based motif searching program Scansite (<http://www.scansite.mit.edu>) [8] to search for proteins that are expressed in adipocytes and contain sequences with high similarity to known Akt/PKB phosphorylation sites. In the present study, we identified TBC1D1 (TBC domain family, member 1) as a potential Akt/PKB substrate in insulin-stimulated 3T3-L1 adipocytes. TBC1D1 is phosphorylated at Thr⁵⁹⁰ within a highly conserved Akt/PKB motif (RRRANT) in cultured adipocytes treated with insulin. Functional analysis revealed that RNAi (RNA interference)-mediated gene silencing of TBC1D1 activates the mTOR-p70 S6 kinase pathway, induces protein expression of the glucose transporter GLUT1 and increases basal glucose transport in adipocytes. These data suggest that the Akt/PKB substrate TBC1D1 may be a negative regulatory element in the insulin signalling pathway of mTOR that regulates GLUT1 protein expression.

EXPERIMENTAL

Materials—Human insulin was obtained from Eli Lilly. Monoclonal antibody against HA (haemagglutinin) epitope 6E2, and rabbit polyclonal antibodies against phospho-Akt/PKB Ser⁴⁷³, phospho-Erk1/2, phospho-S6 ribosomal protein (Ser^{235/236}), phospho-p70 S6 kinase (Thr³⁸⁹), S6 ribosomal protein and phosphorylated Akt/PKB substrate motif were from Cell Signalling Technology. Rabbit polyclonal antibody against Myc epitope was from Upstate Biotechnology. Monoclonal antibody against GLUT4 was from Biogenesis. Rabbit polyclonal antibody against GLUT1 was kindly provided by Dr Paul Pilch (Boston University School of Medicine, Boston, MA, U.S.A.). Rabbit polyclonal antibody against non-muscle myosin IIB was from Covance. Chicken polyclonal antibody against mouse TBC1D4 C-terminus (HPTNDKAKAGNKP) was generated by Quality Controlled Biochemicals, Hopkinton, MA, U.S.A.

Cell culture and electroporation of 3T3-L1 adipocytes—The 3T3-L1 fibroblasts were grown in DMEM (Dulbecco's modified Eagle's medium) supplemented with 10% FBS (fetal bovine serum), 50 µg/ml streptomycin and 50 units/ml penicillin, and differentiated into adipocytes as described [55,56]. The 3T3-L1 adipocytes were transfected with siRNA (small interfering RNA) duplexes or cDNA expression constructs by electroporation as described [56]. Briefly, the adipocytes, on the fourth day of differentiation, were detached from culture dishes with 0.25 % trypsin and 0.5 mg of collagenase/ml in PBS, washed twice and resuspended in PBS. Half of the cells from one 150-mm-diameter dish were then mixed with the indicated siRNA-duplexes or siRNA smart pools, which were delivered to the cells by a pulse of electroporation with a Bio-Rad gene pulser II system at the setting of 0.18 kV and 950 µF capacitance. After electroporation, cells were immediately mixed with fresh media and reseeded into multiple-well plates, designated for Western blotting, RT-PCR (reverse transcription-PCR) or deoxyglucose uptake assay.

siRNAs and constructs—siRNA smart pools and duplexes were synthesized and purified by Dharmacon Research and transfected into the 3T3-L1 fibroblasts and adipocytes by electroporation as described previously [56]. The targeting sequences of each gene are as follows: Akt1/PKB α , AACCAGGACCACGAGAAGCUG; Akt2/PKB β , GAGAGGACCUUCAUGUAG and UGCCAUUCUACAAC-CAGGA. The smart pool siRNAs were used to induce gene-specific silencing of TBC1D1 (M-040360), TBC1D4 (M-040174) and RapGAP220 (M-040315). cDNA expression constructs: cDNAs encoding full-length mouse mKIAA1108 (gi 28972621) and human KIAA0603 (gi 3043729), provided by Kazusa DNA Research Institute, Laboratory for Genome Informatics (Kisarazu, Chiba, Japan), were used to construct full-length TBC1D1 with a Myc epitope fused at the N-terminus (Myc-TBC1D1 WT) and full-length TBC1D4 (AS160) with an HA epitope tag at the N-terminus (HA-TBC1D4 WT), respectively. The mutation Myc-TBC1D1-T590A was made by the PCR-based site-directed mutagenesis.

RT-PCR and real-time PCR analysis of mRNA—Briefly, total RNA was extracted from cells that had been transfected with siRNA using TRIZOL Reagent (Invitrogen). Total RNA was measured by a spectrophotometer and, for RT-PCR, 1 µg of total RNA was used in a cDNA reaction (Invitrogen). PCR was performed on one-tenth of the total cDNA reaction using specific primers of gene(s) of interest and a low number of cycles (< 25). The reactions were run on a gel and percentage of knockdown was estimated by intensity of ethidium bromide-stained bands as compared with scrambled siRNA controls. PCR primers: mouse TBC1D1 forward primer: TCCTTTTGCTC-TGAGGGCATC; reverse primer: TGTGGTCAAGTGCTTCT-GGAGTTC. RapGAP220 forward primer: TGTGAATAACAT-CCAGTCGCCG; reverse primer: CAGCAGCAGTGATAAAG-TCCCC. For quantitative mRNA analysis, 1 µg of total RNA from each sample was used for RT using iScript cDNA

Synthesis kit (Bio-Rad). An aliquot (10%) of each RT reaction was subjected to quantitative real-time PCR analysis using an iQ SYBR green supermix kit and Real-Time PCR detection system following the manufacturers' instructions (MyiQ, Bio-Rad). We designed specific primers using the database PrimerBank (<http://pga.mgh.harvard.edu/primerbank>). HPRT (hypoxanthine–guanine phosphoribosyltransferase) was used as standard housekeeping gene. Relative gene expression was calculated by subtracting the C_t (threshold cycle number) of the target genes from the C_t value of HPRT and squaring this difference (i.e. difference²). Real-time PCR primers used were: TBC1D1 forward primer, GAGCCAACACCCTGAGT-CATT; and reverse primer, GGATTCAAAGTCCTTGCGTTCA. GLUT1 forward primer, CAGTTCGGCTATAACACTGGTG; and reverse primer, GCGCCGACAGAGAAGATG. GLUT4 forward primer, GTGACTGGAACACTGGTCCTA; and reverse primer, CCAGCCACGTTGCATTGTAG.

Immunoprecipitation and immunoblotting—After experimental treatments, the cells were solubilized in ice-cold lysis buffer containing 50 mM Hepes (pH 7.4), 5 mM sodium pyrophosphate, 5 mM β -glycerophosphate, 10 mM sodium fluoride, 2 mM EDTA, 2mM Na_3VO_4 , 1 mM PMSF, 10 $\mu\text{g/ml}$ aprotinin, 10 $\mu\text{g/ml}$ leupeptin and 1 % Triton X-100. Total cell lysates of 1–2 mg of protein were immunoprecipitated with antibodies against phospho-Akt/PKB substrates (1:100 dilution, Cell Signalling), Myc epitope (9E10) or HA epitope (6E2) for 2 h followed by incubation with 80 μl of Protein A-Sepharose 6MB for 2 h at 4 °C. The beads were then washed four times with lysis buffer before boiling for 5 min in Laemmli buffer.

To detect phospho-Akt/PKB substrates, phospho-Ser⁴⁷³ Akt/PKB, phospho-Thr³⁸⁹ p70 S6 kinase, phospho-Thr²⁰²/Tyr²⁰⁴ Erk1/2 and phospho-Ser^{234/236} S6 ribosomal protein, total cell lysates (20 to 50 μg of protein) were resolved with SDS/PAGE and electro-transferred to nitrocellulose membranes, which were incubated with rabbit polyclonal anti-phospho-specific antibodies (1:1000 dilution) overnight at 4°C. Primary chicken antibody against mouse TBC1D4 antibody (1 $\mu\text{g/ml}$), rabbit polyclonal antibodies against total Akt/PKB (1:1000 dilution), GLUT1 (1:10000) and p70 S6 ribosomal protein (1:1000), and mouse monoclonal antibodies against Myc epitope (1:1000), HA epitope (1:1000) and GLUT4 (1:1000) were used to detect their antigens using 20 to 50 mg of proteins from total cell lysates. All the membranes were then incubated with appropriate horseradish peroxidase-linked secondary antibodies (1:10000 dilution each) for 1 h at room temperature (21 °C). The membranes were washed with wash buffer (PBS, pH 7.4, 0.1 % Tween 20) for 1 h at room temperature after incubation with each antibody before detection with ECL[®] (enhanced chemiluminescence) kit.

MS—Proteins immunoprecipitated with PAS antibody were resolved on SDS/PAGE (5–15 % gradient gel) and visualized with a Silver-plus kit according to the procedure recommended by the manufacturer (Bio-Rad). The protein bands were excised from the silver-stained gel and digested with sequencing grade porcine-modified trypsin (Promega). The tryptic peptides were analysed by MALDI–TOF (matrix-assisted laser-desorption ionization-time-of-flight) mass spectrometry as described previously [27]. The peptide mass spectrum was acquired over the range 500–3500 Da. Peptide mass mapping was carried out against the NCBI (National Center for Biotechnology Information) database using the MS-FIT program (University of California, San Francisco, CA, U.S.A.; <http://prospector.ucsf.edu>). To verify further the MS-FIT identification, selected peptides were fragmented via PSD (post-source decay) and searched against the NCBI database using the MStag program.

Deoxyglucose uptake assay—To detect the effect of specific gene silencing on insulin-stimulated glucose transport, [³H]deoxyglucose uptake assays were carried out in 3T3-L1 adipocytes as described previously [17]. Briefly, siRNA-transfected cells were reseeded on 24-well plates and cultured for 72 h before serum starvation for 3 h with KRH (Krebs-ringer Hepes) buffer (130 mM NaCl, 5 mM KCl, 1.3 mM CaCl_2 , 1.3 mM MgSO_4 , 25 mM Hepes,

pH 7.4) supplemented with 0.5 % BSA and 2 mM sodium pyruvate. Cells were then stimulated with insulin for 30 min at 37 °C. Glucose uptake was initiated by addition of [1,2-³H]2-deoxy-D-glucose to a final assay concentration of 100 μM for 5 min at 37 °C. Assays were terminated by four washes with ice-cold KRH buffer and the cells were solubilized with 0.4 ml of 1 % Triton X-100, and radioactivity was determined by scintillation counting. Non-specific deoxyglucose uptake was measured in the presence of 20 μM cytochalasin B and was subtracted from each determination to obtain specific uptake.

RESULTS

Insulin stimulates phosphorylation of multiple GAPs detected by PAS

antibodies—Many studies have reported that PAS antibodies recognize the phosphorylated Akt/PKB substrate motif RXXXXpS/T in target proteins of the kinase [27,30,54]. To identify new Akt/PKB substrates, total cell lysates from control and insulin-stimulated 3T3-L1 adipocytes were immunoprecipitated with PAS antibody and separated by SDS/PAGE, followed by silver staining. Protein bands were excised and subjected to in-gel trypsin digestion. The peptides produced were analysed by MALDI-TOF MS. As shown in Figure 1 (A), immunoprecipitation with PAS antibodies enriched several phosphoproteins detectable by Western blotting with PAS antibodies and silver staining from insulin-stimulated cells. From these silver-stained protein bands, we identified several Akt substrates such as WNK1 and FOXO1 [18]. Interestingly, we also detected several GAPs, including known Akt substrates TBC1D4 (AS160), TSC2 and a 220 kDa RapGAP domain-containing protein (RapGAP220, GeneID: 381383). An online Scansite motif search (<http://scansite.mit.edu>) revealed that all of these GAPs contain high-stringency Akt substrate motifs as shown in Figure 1(B). To examine whether TBC1D4 is phosphorylated in insulin-stimulated adipocytes, a chicken polyclonal antibody against the mouse C-terminal peptide of TBC1D4 was produced. Using anti-PAS antibodies for immunoprecipitation and anti-TBC1D4 antibody for Western blotting, we observed that insulin stimulated TBC1D4 phosphorylation in adipocytes, whereas the PI3K inhibitor wortmannin inhibited insulin's effect (Figure 1D). Our data confirm the initial previous report that TBC1D4 (AS160) is an Akt substrate in insulin-stimulated 3T3-L1 adipocytes [30].

TBC GAP domain-containing protein TBC1D1 is a novel Akt/PKB substrate—To identify additional potential Akt substrates, we scanned Akt motifs with TBC GAP domain-containing proteins expressed in differentiated 3T3-L1 adipocytes, based on microarray gene profiling data (not shown). Interestingly, we found that the Rab GAP TBC1D1 is expressed in the adipocytes and contains several potential Akt motifs (Figure 1B). Similar to TBC1D4, TBC1D1 contains one TBC GAP domain at the C-terminus, two PTB domains (phosphotyrosine-binding domains) at the N-terminus and four potential Akt substrate motifs, with Thr⁵⁹⁰ revealed as the highest stringency site according to the Scansite motif search. To examine whether insulin stimulates TBC1D1 phosphorylation at this potential Akt site, the adipocytes were transfected with expression vectors encoding either full-length Myc-tagged WT (wild-type) mouse TBC1D1 or the Myc-tagged TBC1D1-T590A mutant. Adipocytes were serum starved 48 h after transfection, then stimulated or not with insulin (100 nM) for 15 min; the cells were lysed and anti-Myc epitope antibody was used to immunoprecipitate Myc-tagged TBC1D1-WT or TBC1D1-T590A mutant proteins for Western blotting with anti-PAS antibody. As shown in Figure 1(C), WT TBC1D1 was significantly phosphorylated in adipocytes incubated with insulin, as detected by anti-PAS. However, insulin-stimulated phosphorylation was not observed in the cells expressing the TBC1D1-T590A mutant, suggesting that the Thr⁵⁹⁰ residue is a unique Akt phosphorylation site on TBC1D1 in cultured adipocytes treated with insulin.

RNAi-induced gene-specific silencing of TBC1D1 increases glucose transport in 3T3-L1 adipocytes—It was reported that Akt-mediated phosphorylation of TBC1D4 is involved in the regulation of insulin-stimulated glucose transporter Glut4 translocation and glucose transport in adipocytes [34–36]. To test whether the novel Akt substrates TBC1D1 and RapGAP220 are required for the process of glucose transport, these proteins were knocked down by RNAi-induced gene-specific silencing. Interestingly, siRNA induced knockdown of TBC1D1 mRNA by approx. 70% (Figures 2B and 2C), which increased deoxyglucose transport by approx. 61% and 30% in cultured adipocytes in the basal and low-dose (1 nM) insulin-stimulated states respectively, as compared with cells treated with scrambled siRNA (Figure 2A). However, no significant difference was observed between glucose transporter activities in the adipocytes transfected with the scrambled and TBC1D1 siRNAs when a maximal dose of insulin (100 nM) was used to stimulate the cells. Surprisingly, we consistently observed that the siRNA-induced silencing of TBC1D4 (AS160), by 80 % at the protein level (as determined by Western blotting with AS160 antibody, Figure 2D), had no effect on basal or insulin-stimulated deoxyglucose transport in 3T3-L1 adipocytes (Figure 2A). Similarly, suppression of the RapGAP220 mRNA as indicated by RT–PCR (Figure 2E) did not alter either the basal or insulin-stimulated deoxyglucose transport.

TBC1D1 functions in the regulation of GLUT1 protein expression—To address the question whether the increase in deoxyglucose transport in the cultured adipocytes with TBC1D1 knockdown is due to changes in the expression levels of glucose transporters, we examined mRNA and protein levels of GLUT1 and GLUT4. As shown in Figures 3(A) and 3 (B), loss of TBC1D1 significantly increased GLUT1 protein levels by about 40%, but did not alter GLUT4 or Akt protein levels as detected by Western blotting, when compared with adipocytes treated with scrambled siRNA. However, the decrease of TBC1D4 had no significant effect on either GLUT1 or GLUT4 protein levels. To discriminate between effects of siRNA-mediated suppression of TBC1D1 on transcription versus translation of GLUT1, we measured GLUT1 mRNA levels using real-time PCR. As shown in Figure 3(C), silencing of TBC1D1 did not change GLUT1 and GLUT4 mRNA levels significantly. These data suggest that TBC1D1 suppresses GLUT1 expression mainly at the post-transcriptional level.

TBC1D1 is a negative regulator of the mTOR/p70 S6 kinase pathway—We next investigated whether TBC1D1 is involved in the regulation of insulin signalling on the protein synthesis pathway. As shown in Figures 4(A) and 4(B), siRNA-induced knockdown of either TBC1D1 or TBC1D4 had no effect on basal or insulin-stimulated phosphorylation of Akt (Ser⁴⁷³) in adipocytes. Quantitatively, suppression of TBC1D1 slightly increased basal ERK (extracellular-signal-regulated kinase) 1/2 phosphorylation, but did not significantly alter insulin-stimulated ERK phosphorylation. Interestingly, suppression of TBC1D1, but not TBC1D4, significantly increased basal phosphorylation of p70 S6 kinase at Thr³⁸⁹, a phosphorylation site induced by activated mTOR. Increased phosphorylation at Thr³⁸⁹ in p70 S6 kinase can lead to its activation [46–48]. Consistent with the increase of p70 S6 kinase activity, we also observed that suppression of TBC1D1 resulted in the increase in phosphorylation of S6 ribosomal protein at Ser^{235/236}, the sites phosphorylated by activated p70 S6 kinase, although the protein levels of S6 ribosomal protein were not altered (Figure 4A, bottom panel). These results strongly suggest that siRNA-induced silencing of TBC1D1 increases the activity of the mTOR pathway. However, the decrease of TBC1D1 did not alter insulin-stimulated phosphorylation of p70 S6 kinase and S6 ribosomal protein (Figures 4A and 4B). In our hands, the effect of TBC1D1 silencing on the mTOR pathway is similar to that observed in adipocytes lacking TSC2 (data not shown), a known Akt substrate and negative regulator of the mTOR pathway. Our data are consistent with the notion that TBC1D1 is a negative regulator of the mTOR/p70 S6 kinase pathway in 3T3-L1 adipocytes. It is possible that insulin signalling phosphorylates and inactivates TBC1D1, leading to activation of the

mTOR pathway. Therefore, knockdown of TBC1D1 may mimic insulin's effect, resulting in the increase of basal phosphorylation of p70 S6 kinase and S6 ribosomal protein without altering insulin's stimulatory effects.

Inhibition of mTOR prevents upregulation of GLUT1 protein expression induced by loss of TBC1D1

—It has been reported that insulin stimulates GLUT1 expression through the mTOR signalling pathway, since inhibition of mTOR with rapamycin completely blocks the insulin effect [57,58]. As described above, we observed that suppression of TBC1D1 leads to both the activation of the mTOR pathway and an increase of GLUT1 protein. Therefore, we tested whether mTOR activity is required for the increase in the GLUT1 protein level in the adipocytes lacking TBC1D1. As shown in Figures 5(A) and 5(C), inhibition of mTOR activity with rapamycin for 8 h did not significantly alter the elevated GLUT1 protein expression induced by the silencing of TBC1D1 (Figure 5B), although phosphorylation of S6 ribosomal protein in the total cell lysate was completely blocked (Figure 5A, second panel). However, treatment of the cells with rapamycin for the last 48 h of the 72 h gene-silencing protocol completely prevented this increase of GLUT1 protein in the cells transfected with TBC1D1 siRNA. The lack of effect of rapamycin over only the last 8 h is not unexpected, given the longer half-life of the GLUT1 protein. As expected, short-term treatment (4 h) with insulin did not significantly change GLUT1 protein levels in the cells transfected with either scrambled or TBC1D1-specific siRNAs.

Overexpression of mutant TBC1D1-T590A blocks insulin-stimulated phosphorylation of p70 S6 kinase

—Further studies were designed to test whether a TBC1D1-T590A mutant lacking the Akt phosphorylation site affects insulin-stimulated activation of mTOR. Since the DNA transfection efficacy is much higher in CHO-T cells (Chinese hamster ovary cells transfected with the human insulin receptor) (~50 %) than in 3T3-L1 adipocytes (<5%), CHO-T cells were used in these experiments. In this protocol, pCMV5 vectors with DNA inserts coding HA-tagged TBC1D4, Myc-tagged TBC1D1-WT or Myc-tagged TBC1D1-T590A were transfected into CHO-T cells by electroporation. Then, 48 h later, serum-starved cells were stimulated with insulin (10 nM) for 20 min before total lysate was prepared for detection of insulin-stimulated phosphorylation of Akt/PKB (Ser⁴⁷³) and p70 S6 kinase (Thr³⁸⁹), as well as the expression of HA-tagged TBC1D4 and Myc-tagged TBC1D1 (Figures 6A and 6B). Quantification of the Western blot analyses revealed that overexpression of TBC1D1-T590A significantly reduced insulin-stimulated phosphorylation of p70 S6 kinase at Thr³⁸⁹, but not phosphorylation of Akt/PKB at Ser⁴⁷³, as compared with the cells expressing TBC1D4 or WT TBC1D1. It is possible that WT TBC1D1 can be phosphorylated and inhibited by insulin so that it cannot prevent insulin-induced activation of the mTOR pathway. However, the Akt phosphorylation site mutant TBC1D1-T590A cannot be phosphorylated and inhibited by activated Akt in insulin-stimulated cells. Therefore, overexpression of the mutant form of TBC1D1 will partially block insulin's effect on phosphorylation of p70 S6 kinase. These data are consistent with the notion that TBC1D1 is a negative regulator of the mTOR pathway and that Akt-induced phosphorylation of the Thr⁵⁹⁰ residue may result in the inactivation of the GAP domain-containing protein and, at least partly, the activation of the mTOR/p70 S6 kinase pathway.

DISCUSSION

Using both mass spectrometry-based proteomics with PAS antibody and Akt phosphorylation motif-based bioinformatics to isolate putative Akt substrate proteins, we could confirm that several GAPs are potential Akt/PKB substrates in insulin-stimulated 3T3-L1 adipocytes. These include the known Akt/PKB substrates TSC2 [28,29,40], TBC1D4 [30], and RapGAP220 [33]. We also identified a novel GAP domain-containing protein, TBC1D1, as a novel Akt/PKB substrate by showing that the expressed protein directly reacts with PAS antibody after

insulin stimulation (Figure 1). A point mutation of the putative Akt phosphorylation site revealed that Rab GAP TBC1D1 is indeed phosphorylated in response to insulin at Thr⁵⁹⁰, as predicted by the Scansite motif search program [8]. A key finding in the present study is that silencing of the RabGAP TBC1D1 increases basal deoxyglucose transport in 3T3-L1 adipocytes (Figure 2). This increase is also observed in the presence of submaximal doses of insulin, but not when maximal concentrations of insulin are present (Figure 2). Loss of TBC1D1 also significantly increases the expression of GLUT1 protein, but not GLUT4 protein, in the cultured adipocytes, suggesting that the upregulation of GLUT1 protein expression probably contributes to the increase in deoxyglucose transport (Figure 3). The data are consistent with the concept that GLUT1 accounts for most of the glucose uptake in unstimulated cells, whereas GLUT4 contributes more to the insulin-stimulated glucose uptake. It is interesting to note that, while we were preparing for this manuscript, a study published recently suggested that TBC1D1 acts similarly to TBC1D4 (AS160) as a negative regulator of insulin-stimulated GLUT4 translocation in 3T3-L1 adipocytes [59]. However, our data also demonstrated that cells with a double knockdown of TBC1D1 and GLUT4 still showed increased basal glucose transport as compared with cells treated with the scrambled and GLUT4 siRNAs together (results not shown). Taken together, our data suggest that the increase of basal glucose transport by siRNA-induced suppression of TBC1D1 is dependent on GLUT1 but not GLUT4.

In the present study, our data also showed that insulin stimulates TBC1D4 (AS160) phosphorylation in adipocytes, as detected by the PAS antibody, confirming previously reported data [30]. To our surprise, suppression of TBC1D4 did not alter either basal or insulin-stimulated deoxyglucose transport, even though about 80% loss of TBC1D4 protein was detected in the cells treated with the TBC1D4 gene-specific siRNA (Figure 2). The effect of silencing of TBC1D4 on glucose transport was repeated more than ten times with different batches of cells and siRNAs. One possible explanation is that the remaining 20% of the RabGAP TBC1D4 or TBC1D1 is enough to function fully as a negative regulator of GLUT4 translocation and glucose transport. Studies correlating levels of expression of shRNA (short hairpin RNA) against this protein are consistent with this idea since only the cells showing greatest knockdown displayed compromised GLUT4 translocation [20]. Although both TBC1D1 and TBC1D4 are Akt substrates in insulin-stimulated adipocytes, our study for the first time provides evidence suggesting that TBC1D1, but not its isoform TBC1D4, is involved in the negative regulation of GLUT1 protein expression and basal glucose transport activity in adipocytes. It is worth noting that both TBC1D1 and TBC1D4 contain two PTB domains, suggesting that they may be potentially involved in the interaction with other phosphoproteins and different cellular functions, such as regulating GLUT1 expression by TBC1D1, as described in the present study, and phagosomal maturation by the TBC1D4–Rab14 pathway, reported recently [60]. Interestingly, it was reported that insulin and AMPK (AMP-activated protein kinase) activators regulate both TBC1D1 and TBC1D4 phosphorylation and that they interact with adaptor protein 14-3-3 differently in cultured L6 myotubes. These data suggest potentially distinct intracellular targeting mechanisms for these GAP domain-containing proteins [61].

Activation of the PI3K pathway by insulin and growth factors leads to Akt/PKB-mediated phosphorylation and inactivation of TSC2 [28,29,40]. Since TSC2 is a GAP for the small GTPase Rheb [37–39], inhibition of TSC2 by Akt/PKB leads to the activation of Rheb. Rheb in turn forms a complex with Raptor and activates mTOR by an unknown mechanism [47, 48]. Active mTOR regulates protein synthesis through phosphorylation of p70 S6 kinase and the translation regulator 4E-BP1. It has been reported that insulin stimulates glucose transporter GLUT1 protein translation through the mTOR pathway since the mTOR specific inhibitor rapamycin prevents this insulin effect [57,58]. Interestingly, in the present study we also observed that the Rab GAP TBC1D1, a novel Akt/PKB substrate, is a negative regulator of

GLUT1 protein expression. In addition, RNAi-induced knockdown of endogenous TBC1D1 increases phosphorylation of p70 S6 kinase at Thr³⁸⁹, a known mTOR phosphorylation site (Figure 4). Loss of TBC1D1 also increases phosphorylation of the p70 S6 kinase substrate S6 ribosomal protein (Figure 4). In contrast, overexpression of the TBC1D1-T590A mutant inhibits insulin-stimulated phosphorylation of p70 S6 kinase at Thr³⁸⁹ (Figure 6). Taken together, our data suggest that TBC1D1, similar to TSC2, is a novel negative regulator of the mTOR pathway. Furthermore, TBC1D1 negatively regulates GLUT1 protein expression through inhibiting the mTOR pathway since inhibition of mTOR with rapamycin blocks the stimulatory effect of TBC1D1 knockdown on GLUT1 protein (Figure 5). These results suggest a new pathway by which Akt mediates glucose transport activity in cultured adipocytes. It will be interesting in future studies to elucidate the molecular mechanism by which TBC1D1 regulates the activity of mTOR.

Abbreviations used

AS160	Akt substrate of 160 kDa
CHO-T cell	Chinese hamster ovary cell transfected with the human insulin receptor
4E-BP1	eukaryotic initiation factor 4E-binding protein 1
eIF	eukaryotic initiation factor
FOXO	forkhead box O
GAP	GTPase-activating protein
GLUT	glucose transporter
HA	haemagglutinin
KRH	Krebs-ringer Hepes
MALDI-TOF	matrix-assisted laser-desorption ionization-time-of-flight
mTOR	mammalian target of rapamycin
PAS	phospho-Akt/PKB substrate
PI3K	phosphoinositide 3-kinase
PKB	protein kinase B
PTB domain	phosphotyrosine-binding domain
RNAi	RNA interference
siRNA	small interfering RNA
RT-PCR	reverse transcription-PCR
TBC	Tre-2/Bub2/Cdc16
TBC1D1	TBC domain family, member 1
TBC1D4	TBC domain family, member 4
TSC	tuberous sclerosis complex
WNK1	protein kinase with no lysine 1
WT	wild-type

Acknowledgments

This work was supported by an American Diabetes Association Junior Faculty Award to Z. Y. J. and a National Institutes of Health Grant DK30648 to M. P.C.

REFERENCES

1. Luo J, Manning BD, Cantley LC. Targeting the PI3K-Akt pathway in human cancer: rationale and promise. *Cancer Cell* 2003;4:257–262. [PubMed: 14585353]
2. Brazil DP, Yang ZZ, Hemmings BA. Advances in protein kinase B signalling: AKTion on multiple fronts. *Trends Biochem. Sci* 2004;29:233–242. [PubMed: 15130559]
3. Whiteman EL, Cho H, Birnbaum MJ. Role of Akt/protein kinase B in metabolism. *Trends Endocrinol. Metab* 2002;13:444–451. [PubMed: 12431841]
4. Saltiel AR, Kahn CR. Insulin signalling and the regulation of glucose and lipid metabolism. *Nature* 2001;414:799–806. [PubMed: 11742412]
5. Sarbassov DD, Guertin DA, Ali SM, Sabatini DM. Phosphorylation and regulation of Akt/PKB by the rictor-mTOR complex. *Science* 2005;307:1098–1101. [PubMed: 15718470]
6. Alessi DR, Caudwell FB, Andjelkovic M, Hemmings BA, Cohen P. Molecular basis for the substrate specificity of protein kinase B; comparison with MAPKAP kinase-1 and p70 S6 kinase. *FEBS Lett* 1996;399:333–338. [PubMed: 8985174]
7. Obata T, Yaffe MB, Leparo GG, Piro ET, Maegawa H, Kashiwagi A, Kikkawa R, Cantley LC. Peptide and protein library screening defines optimal substrate motifs for AKT/PKB. *J. Biol. Chem* 2000;275:36108–36115. [PubMed: 10945990]
8. Yaffe MB, Leparo GG, Lai J, Obata T, Volinia S, Cantley LC. A motif-based profile scanning approach for genome-wide prediction of signaling pathways. *Nat. Biotechnol* 2001;19:348–353. [PubMed: 11283593]
9. Brunet A, Bonni A, Zigmond MJ, Lin MZ, Juo P, Hu LS, Anderson MJ, Arden KC, Blenis J, Greenberg ME. Akt promotes cell survival by phosphorylating and inhibiting a Forkhead transcription factor. *Cell* 1999;96:857–868. [PubMed: 10102273]
10. Kops GJ, de Ruiter ND, De Vries-Smits AM, Powell DR, Bos JL, Burgering BM. Direct control of the Forkhead transcription factor AFX by protein kinase B. *Nature* 1999;398:630–634. [PubMed: 10217147]
11. Rena G, Guo S, Cichy SC, Unterman TG, Cohen P. Phosphorylation of the transcription factor forkhead family member FKHR by protein kinase B. *J. Biol. Chem* 1999;274:17179–17183. [PubMed: 10358075]
12. Biggs WH 3rd, Meisenhelder J, Hunter T, Cavenee WK, Arden KC. Protein kinase B/Akt-mediated phosphorylation promotes nuclear exclusion of the winged helix transcription factor FKHR1. *Proc. Natl. Acad. Sci. U.S.A* 1999;96:7421–7426. [PubMed: 10377430]
13. Datta SR, Dudek H, Tao X, Masters S, Fu H, Gotoh Y, Greenberg ME. Akt phosphorylation of BAD couples survival signals to the cell-intrinsic death machinery. *Cell* 1997;91:231–241. [PubMed: 9346240]
14. Ozes ON, Mayo LD, Gustin JA, Pfeffer SR, Pfeffer LM, Donner DB. NF- κ B activation by tumour necrosis factor requires the Akt serine-threonine kinase. *Nature* 1999;401:82–85. [PubMed: 10485710]
15. Romashkova JA, Makarov SS. NF- κ B is a target of AKT in anti-apoptotic PDGF signalling. *Nature* 1999;401:86–90. [PubMed: 10485711]
16. Rommel C, Clarke BA, Zimmermann S, Nunez L, Rossman R, Reid K, Moelling K, Yancopoulos GD, Glass DJ. Differentiation stage-specific inhibition of the Raf-MEK-ERK pathway by Akt. *Science* 1999;286:1738–1741. [PubMed: 10576741]
17. Mayo LD, Donner DB. A phosphatidylinositol 3-kinase/Akt pathway promotes translocation of Mdm2 from the cytoplasm to the nucleus. *Proc. Natl. Acad. Sci. U.S.A* 2001;98:11598–11603. [PubMed: 11504915]
18. Zhou BP, Liao Y, Xia W, Zou Y, Spohn B, Hung MC. HER-2/neu induces p53 ubiquitination via Akt-mediated MDM2 phosphorylation. *Nat. Cell Biol* 2001;3:973–982. [PubMed: 11715018]

19. Liang J, Zubovitz J, Petrocelli T, Kotchetkov R, Connor MK, Han K, Lee JH, Ciarallo S, Catzavelos C, Beniston R, et al. PKB/Akt phosphorylates p27, impairs nuclear import of p27 and opposes p27-mediated G1 arrest. *Nat. Med* 2002;8:1153–1160. [PubMed: 12244302]
20. Shin I, Yakes FM, Rojo F, Shin NY, Bakin AV, Baselga J, Arteaga CL. PKB/Akt mediates cell-cycle progression by phosphorylation of p27(Kip1) at threonine 157 and modulation of its cellular localization. *Nat. Med* 2002;8:1145–1152. [PubMed: 12244301]
21. Viglietto G, Motti ML, Bruni P, Melillo RM, D'Alessio A, Califano D, Vinci F, Chiappetta G, Tschlis P, Bellacosa A, et al. Cytoplasmic relocation and inhibition of the cyclin-dependent kinase inhibitor p27(Kip1) by PKB/Akt-mediated phosphorylation in breast cancer. *Nat. Med* 2002;8:1136–1144. [PubMed: 12244303]
22. Zhou BP, Liao Y, Xia W, Spohn B, Lee MH, Hung MC. Cytoplasmic localization of p21Cip1/WAF1 by Akt-induced phosphorylation in HER-2/neu-overexpressing cells. *Nat. Cell Biol* 2001;3:245–252. [PubMed: 11231573]
23. Fulton D, Gratton JP, McCabe TJ, Fontana J, Fujio Y, Walsh K, Franke TF, Papapetropoulos A, Sessa WC. Regulation of endothelium-derived nitric oxide production by the protein kinase Akt. *Nature* 1999;399:597–601. [PubMed: 10376602]
24. Dimmeler S, Fleming I, Fisslthaler B, Hermann C, Busse R, Zeiher AM. Activation of nitric oxide synthase in endothelial cells by Akt-dependent phosphorylation. *Nature* 1999;399:601–605. [PubMed: 10376603]
25. Cross DA, Alessi DR, Cohen P, Andjelkovich M, Hemmings BA. Inhibition of glycogen synthase kinase-3 by insulin mediated by protein kinase B. *Nature* 1995;378:785–789. [PubMed: 8524413]
26. Vitari AC, Deak M, Collins BJ, Morrice N, Prescott AR, Phelan A, Humphreys S, Alessi DR. WNK1, the kinase mutated in an inherited high-blood-pressure syndrome, is a novel PKB (protein kinase B)/Akt substrate. *Biochem. J* 2004;378:257–268. [PubMed: 14611643]
27. Jiang ZY, Zhou QL, Holik J, Patel S, Leszyk J, Coleman K, Chouinard M, Czech MP. Identification of WNK1 as a substrate of Akt/protein kinase B and a negative regulator of insulin-stimulated mitogenesis in 3T3-L1 cells. *J. Biol. Chem* 2005;280:21622–21628. [PubMed: 15799971]
28. Inoki K, Li Y, Zhu T, Wu J, Guan KL. TSC2 is phosphorylated and inhibited by Akt and suppresses mTOR signalling. *Nat. Cell Biol* 2002;4:648–657. [PubMed: 12172553]
29. Dan HC, Sun M, Yang L, Feldman RI, Sui XM, Ou CC, Nellist M, Yeung RS, Halley DJ, Nicosia SV, Pledger WJ, Cheng JQ. Phosphatidylinositol 3-kinase/Akt pathway regulates tuberous sclerosis tumor suppressor complex by phosphorylation of tuberlin. *J. Biol. Chem* 2002;277:35364–35370. [PubMed: 12167664]
30. Kane S, Sano H, Liu SC, Asara JM, Lane WS, Garner CC, Lienhard GE. A method to identify serine kinase substrates. Akt phosphorylates a novel adipocyte protein with a Rab GTPase-activating protein (GAP) domain. *J. Biol. Chem* 2002;277:22115–22118. [PubMed: 11994271]
31. Kovacina KS, Park GY, Bae SS, Guzzetta AW, Schaefer E, Birnbaum MJ, Roth RA. Identification of a proline-rich Akt substrate as a 14-3-3 binding partner. *J. Biol. Chem* 2003;278:10189–10194. [PubMed: 12524439]
32. Burchfield JG, Lennard AJ, Narasimhan S, Hughes WE, Wasinger VC, Corthals GL, Okuda T, Kondoh H, Biden TJ, Schmitz-Peiffer C. Akt mediates insulin-stimulated phosphorylation of Ndr2: evidence for cross-talk with protein kinase C θ . *J. Biol. Chem* 2004;279:18623–18632. [PubMed: 14985363]
33. Gridley S, Lane WS, Garner CW, Lienhard GE. Novel insulin-elicited phosphoproteins in adipocytes. *Cell Signal* 2005;17:59–66. [PubMed: 15451025]
34. Sano H, Kane S, Sano E, Miinea CP, Asara JM, Lane WS, Garner CW, Lienhard GE. Insulin-stimulated phosphorylation of a Rab GTPase-activating protein regulates GLUT4 translocation. *J. Biol. Chem* 2003;278:14599–14602. [PubMed: 12637568]
35. Eguez L, Lee A, Chavez JA, Miinea CP, Kane S, Lienhard GE, McGraw TE. Full intracellular retention of GLUT4 requires AS160 Rab GTPase activating protein. *Cell Metab* 2005;2:263–272. [PubMed: 16213228]
36. Larance M, Ramm G, Stockli J, van Dam EM, Winata S, Wasinger V, Simpson F, Graham M, Junutula JR, Guilhaus M, James DE. Characterization of the role of the Rab GTPase-activating protein AS160

- in insulin-regulated GLUT4 trafficking. *J. Biol. Chem* 2005;280:37803–37813. [PubMed: 16154996]
37. Zhang Y, Gao X, Saucedo LJ, Ru B, Edgar BA, Pan D. Rheb is a direct target of the tuberous sclerosis tumour suppressor proteins. *Nat. Cell Biol* 2003;5:578–581. [PubMed: 12771962]
 38. Garami A, Zwartkruis FJ, Nobukuni T, Joaquin M, Roccio M, Stocker H, Kozma SC, Hafen E, Bos JL, Thomas G. Insulin activation of Rheb, a mediator of mTOR/S6K/4E-BP signaling, is inhibited by TSC1 and 2. *Mol. Cell* 2003;11:1457–1466. [PubMed: 12820960]
 39. Inoki K, Li Y, Xu T, Guan KL. Rheb GTPase is a direct target of TSC2 GAP activity and regulates mTOR signaling. *Genes Dev* 2003;17:1829–1834. [PubMed: 12869586]
 40. Manning BD, Tee AR, Logsdon MN, Blenis J, Cantley LC. Identification of the tuberous sclerosis complex-2 tumor suppressor gene product tuberlin as a target of the phosphoinositide 3-kinase/Akt pathway. *Mol. Cell* 2002;10:151–162. [PubMed: 12150915]
 41. Tee AR, Manning BD, Roux PP, Cantley LC, Blenis J. Tuberous sclerosis complex gene products, Tuberlin and Hamartin, control mTOR signaling by acting as a GTPase-activating protein complex toward Rheb. *Curr. Biol* 2003;13:1259–1268. [PubMed: 12906785]
 42. Martin DE, Hall MN. The expanding TOR signaling network. *Curr. Opin. Cell Biol* 2005;17:158–166. [PubMed: 15780592]
 43. Tee AR, Blenis J. mTOR, translational control and human disease. *Semin. Cell Dev. Biol* 2005;16:29–37. [PubMed: 15659337]
 44. Hay N, Sonenberg N. Upstream and downstream of mTOR. *Genes Dev* 2004;18:1926–1945. [PubMed: 15314020]
 45. Proud CG. Regulation of protein synthesis by insulin. *Biochem. Soc. Trans* 2006;34:213–216. [PubMed: 16545079]
 46. Pearson RB, Dennis PB, Han JW, Williamson NA, Kozma SC, Wettenhall RE, Thomas G. The principal target of rapamycin-induced p70s6k inactivation is a novel phosphorylation site within a conserved hydrophobic domain. *EMBO. J* 1995;14:5279–5287. [PubMed: 7489717]
 47. Avruch J, Hara K, Lin Y, Liu M, Long X, Ortiz-Vega S, Yonezawa K. Insulin and amino-acid regulation of mTOR signaling and kinase activity through the Rheb GTPase. *Oncogene* 2006;25:6361–6372. [PubMed: 17041622]
 48. Reiling JH, Sabatini DM. Stress and mTOR signaling. *Oncogene* 2006;25:6373–6383. [PubMed: 17041623]
 49. Ferrari S, Bandi HR, Hofsteenge J, Bussian BM, Thomas G. Mitogen-activated 70K S6 kinase. Identification of *in vitro* 40 S ribosomal S6 phosphorylation sites. *J. Biol. Chem.* 1991;266:22770–22775.
 50. Ruvinsky I, Meyuhas O. Ribosomal protein S6 phosphorylation: from protein synthesis to cell size. *Trends Biochem. Sci* 2006;31:342–348. [PubMed: 16679021]
 51. Brunn GJ, Hudson CC, Sekulic A, Williams JM, Hosoi H, Houghton PJ, Lawrence JC Jr, Abraham RT. Phosphorylation of the translational repressor PHAS-I by the mammalian target of rapamycin. *Science* 1997;277:99–101. [PubMed: 9204908]
 52. Scott PH, Brunn GJ, Kohn AD, Roth RA, Lawrence JC Jr. Evidence of insulin-stimulated phosphorylation and activation of the mammalian target of rapamycin mediated by a protein kinase B signaling pathway. *Proc. Natl. Acad. Sci. U.S.A* 1998;95:7772–7777. [PubMed: 9636226]
 53. Shah OJ, Anthony JC, Kimball SR, Jefferson LS. 4E-BP1 and S6K1: translational integration sites for nutritional and hormonal information in muscle. *Am. J. Physiol. Endocrinol. Metab* 2000;279:E715–E729. [PubMed: 11001751]
 54. Zhang H, Zha X, Tan Y, Hornbeck PV, Mastrangelo AJ, Alessi DR, Polakiewicz RD, Comb MJ. Phosphoprotein analysis using antibodies broadly reactive against phosphorylated motifs. *J. Biol. Chem* 2002;277:39379–39387. [PubMed: 12151408]
 55. Harrison SA, Buxton JM, Clancy BM, Czech MP. Insulin regulation of hexose transport in mouse 3T3-L1 cells expressing the human HepG2 glucose transporter. *J. Biol. Chem* 1990;265:20106–20116. [PubMed: 2173694]
 56. Jiang ZY, Zhou QL, Coleman KA, Chouinard M, Boese Q, Czech MP. Insulin signaling through Akt/protein kinase B analyzed by small interfering RNA-mediated gene silencing. *Proc. Natl. Acad. Sci. U.S.A* 2003;100:7569–7574. [PubMed: 12808134]

57. Taha C, Liu Z, Jin J, Al-Hasani H, Sonenberg N, Klip A. Opposite translational control of GLUT1 and GLUT4 glucose transporter mRNAs in response to insulin. Role of mammalian target of rapamycin, protein kinase B, and phosphatidylinositol 3-kinase in GLUT1 mRNA translation. *J. Biol. Chem* 1999;274:33085–33091. [PubMed: 10551878]
58. Taha C, Mitsumoto Y, Liu Z, Skolnik EY, Klip A. The insulin-dependent biosynthesis of GLUT1 and GLUT3 glucose transporters in L6 muscle cells is mediated by distinct pathways. Roles of p21ras and pp70 S6 kinase. *J. Biol. Chem* 1995;270:24678–24681.
59. Roach WG, Chavez JA, Miinea CP, Lienhard GE. Substrate specificity and effect on GLUT4 translocation of the Rab GTPase-activating protein Tbc1d1. *Biochem. J* 2007;403:353–358. [PubMed: 17274760]
60. Kuijl C, Savage NDL, Marsman M, Tuin AW, Janssen L, Egan DA, Ketema M, Nieuwendijk RVD, Eeden SJFVD, Geluk A, et al. Intracellular bacterial growth is controlled by a kinase network around PKB/AKT1. *Nature* 2007;450:725–730. [PubMed: 18046412]
61. Chen S, Murphy J, Toth R, Campbell DG, Morrice NA, Mackintosh C. Complementary regulation of TBC1D1 and AS160 by growth factors, insulin and AMPK activators. *Biochem. J* 2008;409:449–459. [PubMed: 17995453]

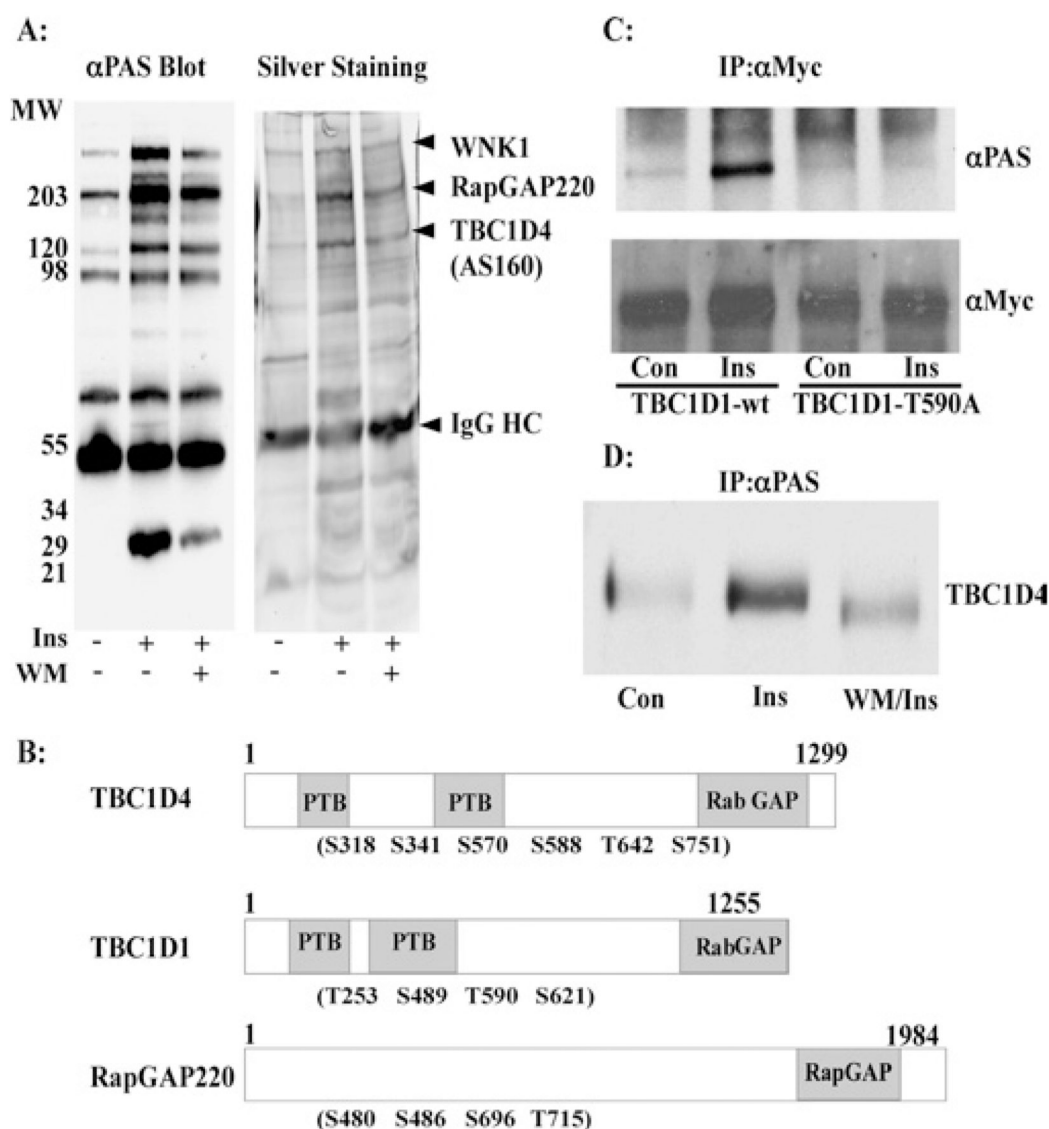


Figure 1. RabGAP domain-containing proteins, TBC1D1 and TBC1D4, are Akt substrates
(A) Serum-starved 3T3-L1 adipocytes were treated with or without 100 nM wortmannin (WM) for 20 min followed by incubation with or without 100 nM insulin (Ins) for 15 min. Total cell lysate (6 mg of protein) was used for immunoprecipitation with PAS antibody as described in the Experimental section. Protein bands on SDS/PAGE (5–15% gel) were blotted with PAS antibody and visualized by silver staining. The protein bands were excised and digested in the gel with trypsin and the tryptic peptides were analysed with a MALDI-TOF mass spectrometer. The identified proteins are indicated. **(B)** Schematic diagram of mouse TBC1D1, TBC1D4 and RapGAP220. The domains predicted by the Pfam program and potential Akt/PKB phosphorylation sites are shown. **(C and D)** Akt/PKB phosphorylates WT TBC1D1 and TBC1D4, but not TBC1D1-T590A. 3T3-L1 adipocytes were transfected with Myc-tagged TBC1D1 WT and TBC1D1-T590A. Con, control. **(C)** Myc-tagged proteins were immunoprecipitated (IP) from the indicated cell lysates with anti-Myc polyclonal antibody (αMyc). Samples were then resolved by SDS/PAGE and immunoblotted with anti-PAS antibody (αPAS). The anti-Myc (αMyc) blot is also shown as control. **(D)** 3T3-L1 adipocyte lysates were immunoprecipitated (IP) with anti-PAS antibody (αPAS) and samples were

resolved by SDS/PAGE and immunoblotted with anti-TBC1D4 antibody. Data are representative of three independent experiments.

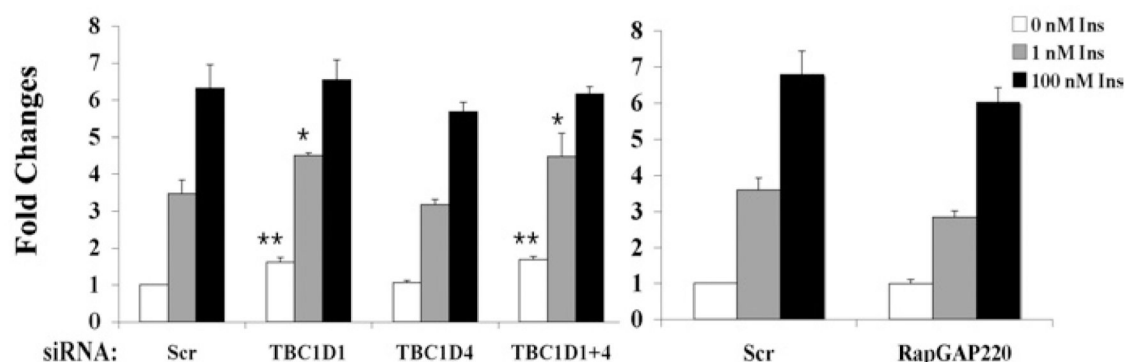
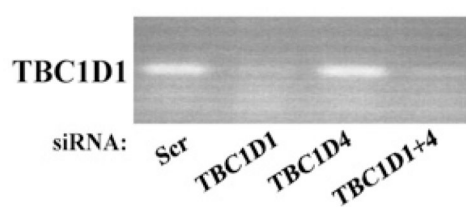
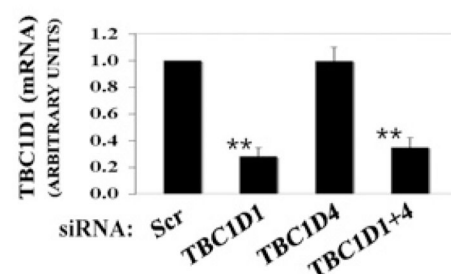
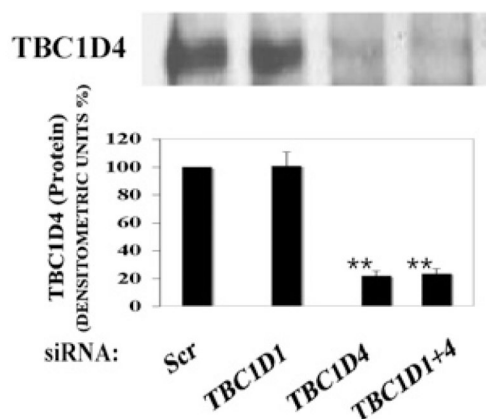
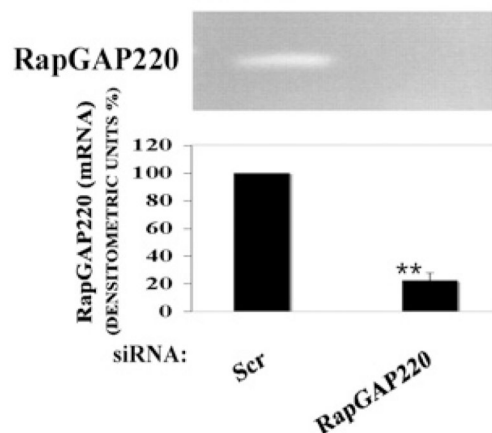
A: DEOXYGLUCOSE UPTAKE:**B: RT-PCR:****C: REAL-TIME PCR:****D: WESTERN BLOT:****E: RT-PCR:**

Figure 2. Gene silencing of TBC1D1, but not TBC1D4 or RapGAP220, increases glucose transport in 3T3-L1 adipocytes

3T3-L1 adipocytes were transfected with the indicated siRNAs (10 nmol) by electroporation and reseeded and incubated for 72 h. Scr, scrambled. (A) Comparison of insulin-stimulated [3 H]deoxyglucose uptake by adipocytes transfected with different siRNAs. The serum-starved cells were stimulated by 1 or 100 nM insulin and the deoxyglucose uptake was assayed as described in the Experimental section. (B, C and E) siRNA-induced gene silencing. Total RNA was extracted from cells transfected with siRNAs as indicated using TRIZOL reagent. Agarose gel images of RT-PCR and real-time PCR results show TBC1D1 (B and C) and RapGAP220 (E) mRNA knockdowns. (D) Western blot shows TBC1D4 protein knockdown by siRNA.

Cell lysates were prepared and 30 µg of protein from each sample was resolved by SDS/PAGE and immunoblotted with anti-TBC1D4 antibody. Data are presented as the mean \pm S.E.M. of five independent experiments and the unpaired Student's *t* test showed $*P < 0.05$ and $**P < 0.005$ for differences between cells transfected with scrambled siRNA against cells transfected with siRNAs as indicated.

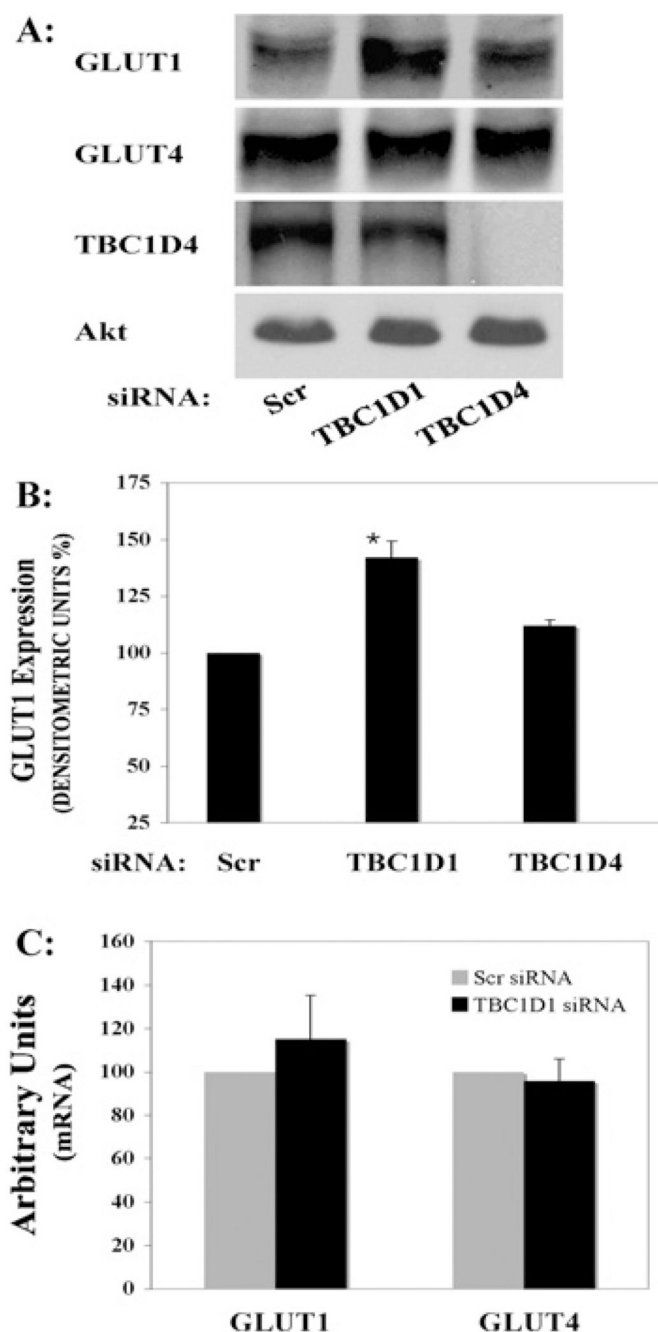
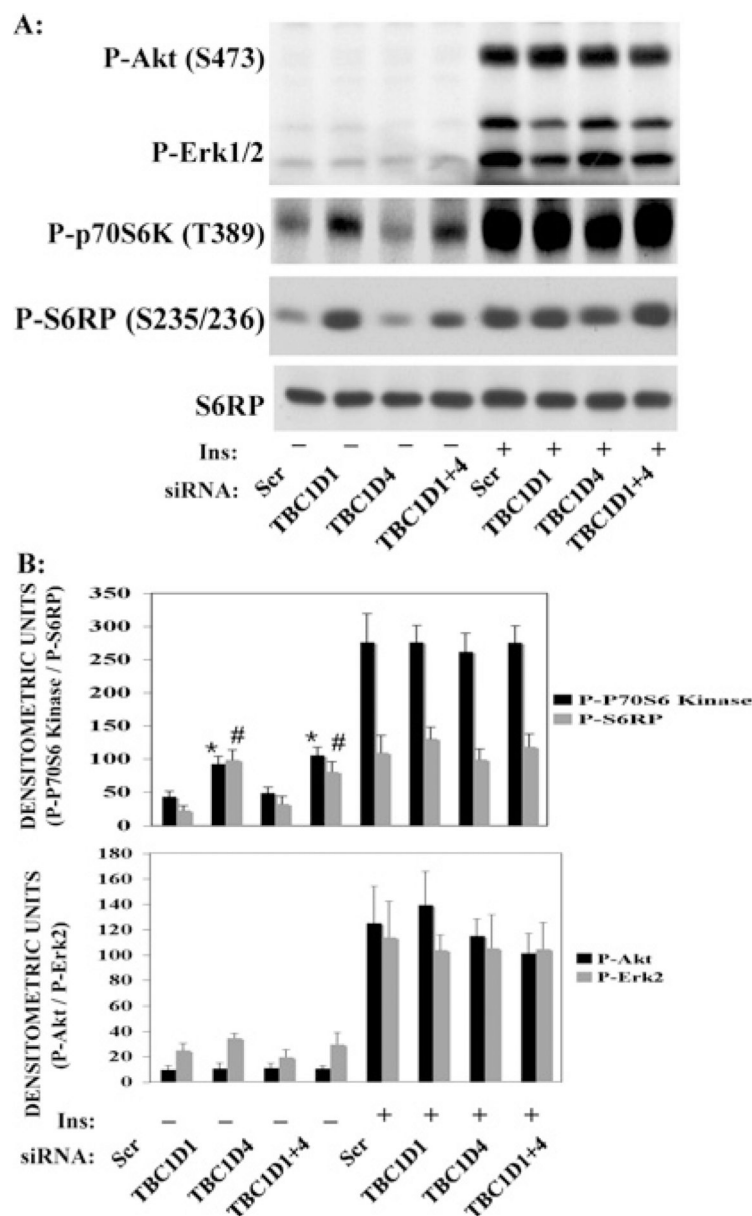


Figure 3. Gene silencing of TBC1D1 enhances GLUT1 protein but not gene expression in 3T3-L1 adipocytes

3T3-L1 adipocytes were transfected with the indicated siRNA (10 nmol) by electroporation, reseeded and incubated for 72 h. (A) Cell lysates were prepared and 30 μ g of protein from each sample was resolved by SDS/PAGE and immunoblotted with anti-GLUT1, anti-GLUT4, anti-TBC1D4 and anti-Akt antibodies. (B) Protein bands of GLUT1 expression were scanned and intensities were determined by densitometry using the Adobe Photoshop CS2 software program. (C) Total RNA was extracted from cells transfected with the indicated siRNAs using TRIZOL reagent and real-time PCR results show mRNA levels of GLUT1 and GLUT4. Data

are presented as the mean \pm S.E.M. of three independent experiments and $*P < 0.005$ as compared with the scrambled (Scr) siRNA group.



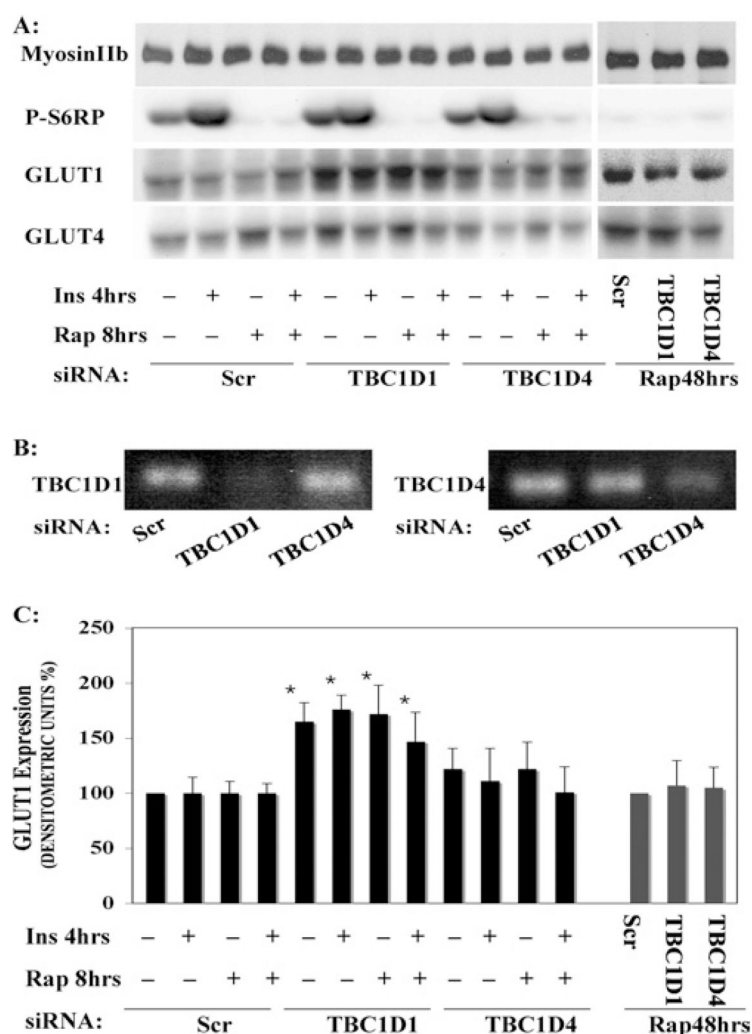


Figure 5. Inhibition of mTOR prevents the increase in GLUT1 protein expression due to the decrease of TBC1D1 in 3T3-L1 adipocytes

3T3-L1 adipocytes were transfected with indicated siRNA (10 nmol) by electroporation, reseeded and incubated for 72 h. (A) The cells were then treated with or without 20 nM rapamycin (Rap) for 8 h or 48 h, then with or without 100 nM insulin (Ins) for 4 h. Total cell lysates were prepared and 20 µg of protein from each sample was resolved by SDS/PAGE and immunoblotted with antibodies as indicated. P-S6RP, phospho-S6 ribosomal protein. (B) Agarose gel images show the results of the PCR analysis of TBC1D1 and TBC1D4 mRNA knockdowns. (C) Protein bands of GLUT1 expression were scanned and intensities were determined by densitometry using the Adobe Photoshop CS2 software program. Data are presented as the mean ± S.E.M. of three independent experiments and * $P < 0.005$ as compared with the scrambled (Scr) siRNA groups.

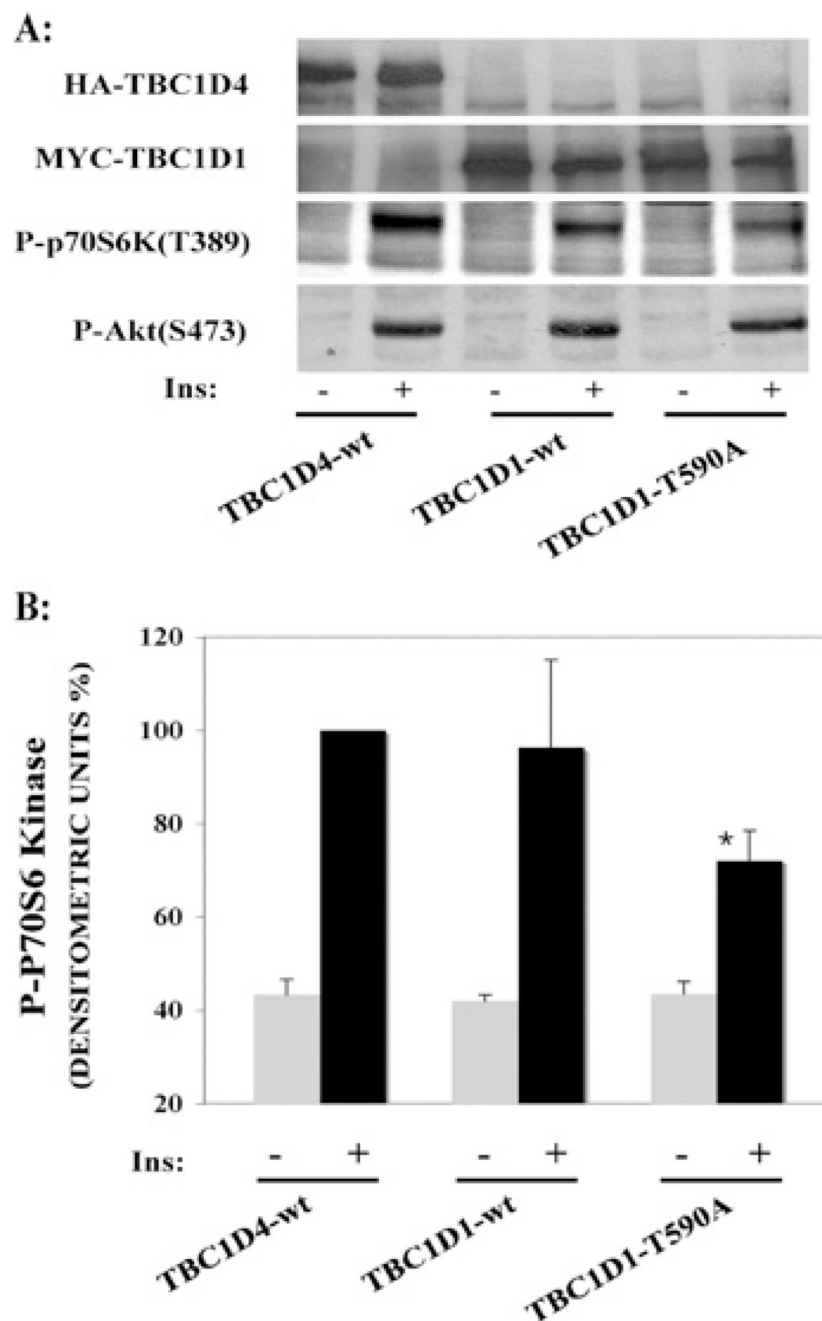


Figure 6. Mutation of TBC1D1 at the Akt phosphorylation site inhibits the activation of the mTOR-p70 S6 kinase pathway in CHO-T cells

CHO-T cells were transfected with Myc-tagged TBC1D1-WT, Myc-tagged TBC1D1-T590A and HA-tagged TBC1D4-WT by electroporation, reseeded and incubated for 48 h. The cells were then treated with or without insulin (Ins; 10 nM) for 30 min. (A) Total cell lysates were prepared and 30 μ g of protein from each sample was resolved by SDS/PAGE and immunoblotted with antibodies as indicated. P-Akt, phospho-Akt; P-p70S6K, phospho-p70 S6 kinase. (B) Protein bands of phospho-p70 S6 kinase were scanned and intensities were determined by densitometry using the Adobe Photoshop CS2 software program. Data are

presented as the mean \pm S.E.M. of three independent experiments and $*P < 0.005$ as compared with the TBC1D4 WT group.